

# Anisotropic Molecular Ionization at 1 V from Tellurium Nanowires (Te NWs)

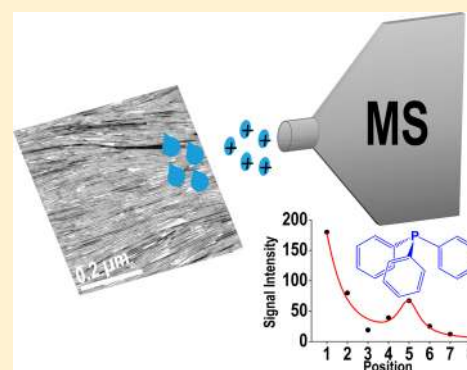
Rahul Narayanan,<sup>†</sup> Depanjan Sarkar,<sup>†</sup> Anirban Som,<sup>†</sup> Michael Wlekinski,<sup>‡</sup> R. Graham Cooks,<sup>\*,†,‡</sup> and Thalappil Pradeep<sup>\*,†</sup>

<sup>†</sup>DST Unit of Nanoscience (DST UNS) and Thematic Unit of Excellence (TUE), Department of Chemistry, Indian Institute of Technology Madras, Chennai 600036, India

<sup>‡</sup>Department of Chemistry, Purdue University, West Lafayette, Indiana 47907, United States

## S Supporting Information

**ABSTRACT:** Ionization of molecular species from one-dimensional (1D) tellurium nanowires (Te NWs) has been achieved at 1 V. Molecules with a range of chemical functional groups gave quality mass spectra with high signal/noise ratios and no fragment ions. Experiments suggest the possibility of emission of microdroplets of solution due to the intense fields at the ends or interfaces of nanostructures. It appears that electrolytic conduction of the solution wetting of the nanostructures and not the electronic conduction of the nanostructures themselves is involved in the ionization event. Anisotropy was seen when two-dimensionally aligned Te NWs were used for ionization. The orientation effect of aligned Te NWs on molecular ion intensity is demonstrated for many analytes including organic molecules and amino acids with experiments done using a silicon substrate having aligned Te NWs. These measurements suggest the possibility of creating a MS source that extends the applicability of mass spectrometry. Analysis of a variety of analytes, including amino acids, pesticides, and drugs, in pure form and in complex mixtures, is reported. These experiments suggest that 1D nanostructures in general could be excellent ionization sources.



Creation of molecular ions using the high electric fields associated with the application of electrical potentials to small objects is embodied in the methods of field ionization (FI) and field desorption (FD) mass spectrometry.<sup>1,2</sup> These ionization methods, although still in use,<sup>3</sup> inconveniently involve unit operations in a vacuum. The development of ambient ionization methods which employ unmodified samples in the open air<sup>4–13</sup> has led to ionization from solutions on paper substrates<sup>14–18</sup> by application of voltages in the low kV range. Addition of carbon nanotubes to the paper substrate<sup>19</sup> yields mass spectra with the application of just 3 V. Recently these MS techniques have found a significant role in the study of various biologically important systems also.<sup>20,21</sup>

We now show that (i) one-dimensional (1D) aligned tellurium nanowires (Te NWs) supported on a suitable substrate give mass spectra with high signal/noise ratios upon application of just 1 V and that (ii) ion emission is strongly anisotropic, the orientation of the support relative to the inlet of the mass spectrometer exerting a strong effect on ion intensity as a result of preferential orientation of the Te NWs. The data suggest that solution-phase emission of charged microdroplets occurs and that electrolytic conduction over the nanostructures is responsible for this effect.

Tellurium is a semiconducting material which has high inherent tendency for anisotropic growth.<sup>22</sup> One-dimensional (1D) nanowires of Te can be prepared with ease, in solution.<sup>23</sup>

These nanowires can be aligned over a substrate, and this property is utilized for the measurements outlined here. In particular, the high electric fields associated with the nanowires even at low applied voltages facilitate ionization.

## EXPERIMENTAL SECTION

**Materials.** The chemicals used for the synthesis of aligned Te NWs (TeO<sub>2</sub>, NaOH, PVP, ammonia solution, N<sub>2</sub>H<sub>4</sub>·H<sub>2</sub>O, and butanol) were purchased from Sigma-Aldrich, India. The medicinal tablets used in these experiments were purchased from a local pharmacy. All the amino acids were bought from Sisco Research Laboratories Pvt. Ltd., Mumbai, India. The pesticides were purchased from Sigma-Aldrich, India. Triphenylphosphine and tributylphosphine were bought from Spectrochem Pvt. Ltd., Mumbai, India and Wako Pure Chemical Industries Ltd., respectively. Diphenylamine (DPA) and triethylamine were from Merck Ltd., Mumbai, India. The salts for the preformed ion study were purchased from Sigma-Aldrich, India.

**Synthesis of Te NWs.** A well-known synthetic strategy was modified for the preparation of Te NWs.<sup>22</sup> For this, a TeO<sub>2</sub> solution was prepared by dissolving 66.3 mg of TeO<sub>2</sub> in a basic

Received: April 28, 2015

Accepted: October 11, 2015

Published: October 11, 2015

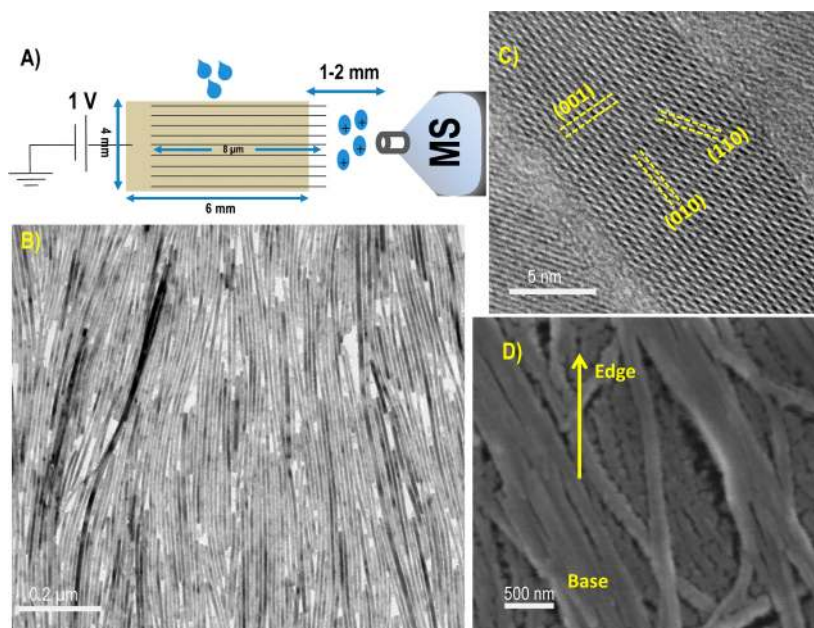


**Figure 1.** (A) Schematic of the ionization process (include appropriate scale bars), (B) low magnification TEM image of aligned Te NWs, (C) high magnification HRTEM image of TE NWs, and (D) FE SEM image of aligned Te NWs-coated paper clamped onto carbon tape. Various lattice planes observed are marked in C. The edge of the paper substrate is marked in D. The NWs coat the surface uniformly and a thin coating visibly changes the color of the paper. In panels B and C, copper grids were used as substrates.

medium containing 0.3 g of NaOH in 2 mL of distilled water. This solution was mixed with a polyvinylpyrrolidone (PVP) solution containing 500 mg of PVP (30 kDa) in 30 mL of distilled water in a Teflon-lined stainless steel autoclave. To this, 2.5 mL of ammonia and 500  $\mu\text{L}$  of 99%  $\text{N}_2\text{H}_4\cdot\text{H}_2\text{O}$  were added and stirred for 15 min. The reaction was kept at 180  $^\circ\text{C}$  for 3 h. A dark blue colored Te NWs suspension was obtained from which the Te NWs were precipitated by centrifugation. The NWs were characterized by transmission electron microscopy (10  $\mu\text{m}$  long wires of  $\sim 10\text{--}12$  nm diameter) and by optical absorption spectroscopy.

**Freestanding Aligned Layers of Te NWs.** The freshly synthesized ultrathin Te NWs were washed thoroughly by centrifuging at 20 000 rpm, and the pellet was dispersed in 1 mL of n-butanol. The resulting suspension was carefully added dropwise to water in a Petri dish to form a thin bluish layer of NWs (8  $\mu\text{m}$  length and 10 nm diameter) between the water–butanol interface due to their buoyancy and capillary forces.<sup>23</sup> A schematic illustration of NWs alignment is shown in Figure S1. A TEM grid was placed upside down over the surface to capture the NW layer, which was dried and characterized under TEM. The aligned nanostructures can be transferred to other substrates such as a silicon (001) single crystal surface, which were used for the ionization anisotropy experiments discussed later in the paper.

For most experiments, the so-prepared aligned tellurium nanowire suspension in butanol was transferred directly onto a piece of Whatman 42 filter paper. For this, the filter paper was held parallel over the surface of the NW suspension in the Petri dish and the suspension was transferred carefully to the paper (by moving the substrate along the water–butanol interface). The paper was dried under laboratory conditions at room temperature and cut using a pair of scissors in a rectangular shape in dimensions of  $4 \times 6$  mm (base  $\times$  height). In the case of Si, a pre-cut substrate (by using a diamond knife) was used to deposit the Te NWs. It was mounted on a copper clip and held

in front of the mass spectrometer (MS) inlet at a distance of  $\sim 1\text{--}2$  mm. This distance was set manually and was not precisely controlled. The copper clip was connected to an external voltage supply, and a voltage of 1 V was applied for all the measurements except when indicated otherwise. The paper was not cut in the triangular shape typically used in paper spray ionization to ensure that the enhanced fields at the (macroscopic) corners of the triangular paper tip did not cause an artifact in the measurement of effects associated with the microscopic NW features. Many samples were analyzed including amino acids, pesticides, and commercial medical tablets. All samples (2  $\mu\text{L}$ ) were used at a concentration of 50 ppm. For all the experiments, HPLC grade methanol (Sigma-Aldrich) and methanol/water (1:1 by volume) were used as solvents. All the mass spectra were recorded at 1 V in positive ion mode with negative ion mode data also being acquired when analyzing preformed ions. The following experimental conditions were maintained for all the measurements: source voltage:  $\pm 1$  V; capillary temperature: 150  $^\circ\text{C}$ ; capillary voltage: 0 V; and tube lens voltage: 0 V.

**Techniques.** All the measurements were made using an ion trap LTQ XL (Thermo Scientific, San Jose, California). Collision-induced dissociation was used for MS<sup>2</sup> analysis. A field emission scanning electron microscope (FE SEM) was used for imaging of the paper. Raman measurements were made using a Witec GmbH Confocal Raman Microspectrometer, Germany with 532 and 633 nm laser excitation sources.

## RESULTS AND DISCUSSION

Suitably cut Te NWs-coated paper was supplied with the desired potential, delivered from a power supply, and the modified paper was mounted in front of the MS inlet for the current experiments. A schematic of the process is shown in Figure 1A. Here a rectangular piece of paper was held in front of the MS inlet at a distance of  $\sim 1\text{--}2$  mm. The shape of the paper is unimportant in the measurements. Normal paper

(without NWs) does not give detectable ion signals below 500 V (Figure S2B). Various analytes in methanol/water (1:1) at a concentration of 50 ppm were added onto the paper with a micropipette. About 2  $\mu\text{L}$  of sample (i.e.,  $10^{-7}$  g, absolute) was used for a single measurement. Under these conditions, the aligned Te NW paper gave ions which were analyzed using an ion trap LTQ XL mass spectrometer. The rectangularly cut paper was examined with a field emission scanning electron microscope (FE SEM). The image, shown in Figure 1D, revealed the presence of aligned Te NWs on the paper. The corresponding low magnification TEM and HRTEM images of Te NWs on a standard copper grid display the same features, as shown in Figure 1B and 1C.

A fascinating feature of ionization at low voltage is the presence of  $[\text{M} + \text{H}]^+$  ( $\text{M}$  = molecule) without any fragment ions. These low voltage mass spectra are characterized by their high signal/noise ratios. Such a low voltage (1 V) mass spectrum of DPA is shown in Figure 2A. The figure represents

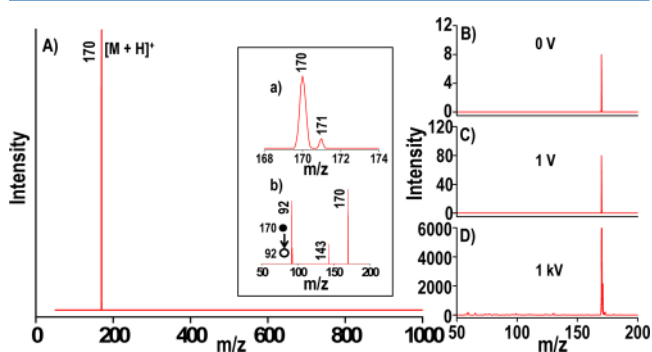


**Figure 2.** (A) Full scan mass spectrum of 100 ng DPA with inset showing isotopic distribution of the molecular ion peak (a) and MS<sup>2</sup> of molecular ion peak (b). (B), (C), and (D) show mass spectra of DPA at 0 V, 1 V and 1 kV, respectively. There are processes which give minor signals even at 0 V.

a full range mass spectrum which was collected at 1 V by applying 50 ppm of DPA in methanol/water to the substrate. The volume of the sample solution used for a single experiment was 2  $\mu\text{L}$  (corresponding to 100 ng, absolute). Typically, 50 scans were recorded and averaged from this quantity of analyte. The spectrum is characterized by the presence of the protonated molecule at  $m/z$  170 with a well-defined isotopic distribution (shown in the inset). The identity of the protonated molecule was confirmed by MS-MS analysis, which is also shown as an inset. The expected benzene loss product was seen at  $m/z$  92. The results are shown in Figure 2B and Figure 2C, which represent the mass spectrum of diphenylamine at 0 and 1 V, respectively. (There are processes which can give minor signal even at 0 V, but these depend on the experimental and atmospheric conditions.) For comparison, the mass spectrum of diphenylamine at 1 kV (using the same Te NWs-coated paper) is shown in Figure 2D. This has a more noisy background and lower signal/noise ratio than the mass spectrum at 1 V. The variation of S/N ratio as a function of voltage is depicted in Figure S2C. It is important to note that the signal at 1 V is  $10^2$  times smaller than that at 1 kV. This is an approximation made, as signal intensity is a function of many factors (substrate to MS inlet distance, capillary voltage, capillary temperature, etc.). Integration time for 1 V and 1 kV spectra are 0.4 and 1.5 min, respectively.

The role of aligned nanostructures (Te NWs) in ejecting ions at 1 V has been verified by conducting the same experiment with similarly cut Whatman 42 filter paper (without Te NWs on it). This paper did not give any ions at low voltage demonstrating that 1D nanostructures can act as electrodes that eject ions even at 1 V. The threshold voltage for ion ejection from Whatman 42 filter paper of the same shape and placement without NWs was tested with various analytes and a minimum of 400–500 V was found to be necessary for ejecting ions. The results are shown in Figure S2A and Figure S2B, which represent the mass spectra of DPA from normal Whatman 42 filter paper at 500 V and below 500 V, respectively. The dependence of signal intensity on voltage was tested with nanowire-coated paper and normal Whatman 42 filter paper. The results are shown in Figure S2D and Figure S2E, respectively. Here DPA at 50 ppm was analyzed at various voltages starting from 1 V to 5 kV (for nanowire-coated paper). The data showed an enhancement in signal intensity with increasing voltage, plateauing at 3 kV. Similar results were obtained for normal Whatman filter paper also.

Ionization at 3 V from protruding carbon nanotubes has been suggested to follow a “field ionization of microdroplet” mechanism.<sup>24,25</sup> The main feature of this mechanism is that ionization occurs in the solution phase. This was supported by various experimental data. The present data also support solution-phase ionization and emission of charged microdroplets. The key role of solvent in the ionization at 1 V was tested with various amines and phosphines by varying the pH. Two amines (diphenylamine and triethylamine) and two phosphines (triphenylphosphine and tributylphosphine) were selected, and mass spectra of these analytes were recorded before and after the addition of dilute acid (HCl). The results are shown in Figure 3. The results show an enhancement in

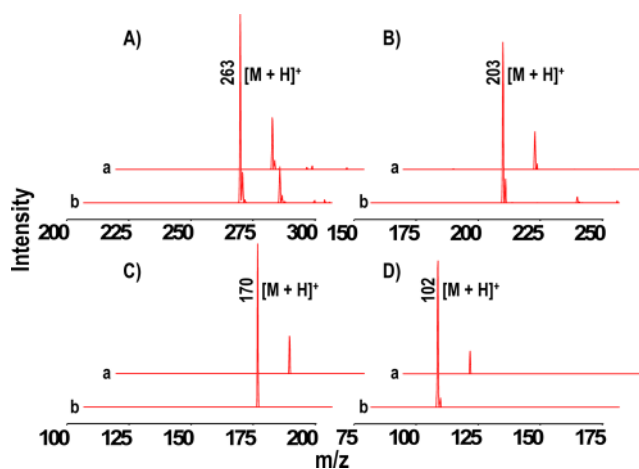


**Figure 3.** Signal intensity enhancement for various analytes (a, before adding HCl, and b, after adding HCl). (A) Triphenylphosphine, (B) tributylphosphine, (C) diphenylamine, and (D) triethylamine.

intensity of the protonated molecule after the addition of dilute acid (HCl). This reveals the role of solution-phase acid/base equilibria in the ionization process and supports the proposed solution-phase ionization mechanism. This was also supported by another experiment of introducing vapors of a highly volatile analyte species (triethylamine dissolved in acetone) between the tip of the paper and the MS inlet. The absence of a molecular ion peak in this case supports the solution-phase



ionization mechanism and is not consistent with ionization in the gas phase.

Solution-phase ionization at 1 V was further supported by results obtained for salts from which preformed ions of both the polarities are observed in low-voltage mass spectra. Solutions of preformed ions were made in methanol/water (1:1) at a concentration of 50 ppm, and they were introduced onto a rectangularly cut Te NWs-coated paper in volumes of 2  $\mu\text{L}$  at a time (i.e., again in 100 ng amounts). Figure 4 represent

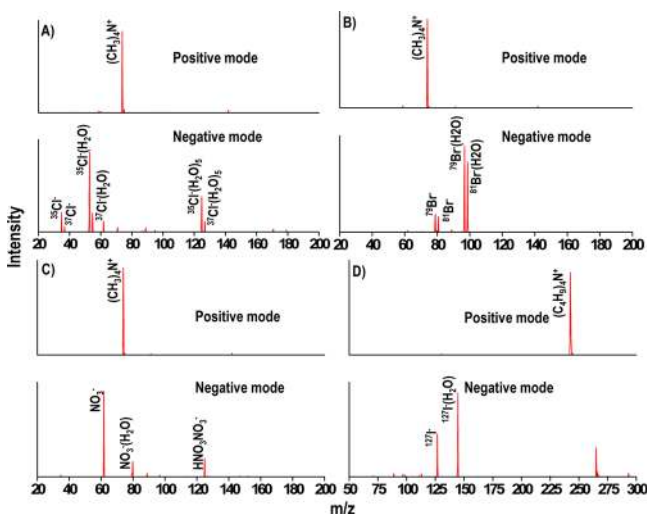


**Figure 4.** Analysis of preformed ions. (A) Tetramethylammonium chloride, (B) tetramethylammonium bromide, (C) tetramethylammonium nitrate, and (D) tetrabutylammonium iodide.

the results obtained. The mass spectra were collected both in positive and negative modes for the positive and negative counterions, respectively. These experiments also substantiate solution-phase ionization via microdroplet emission.

To evaluate the structural and chemical changes that might have occurred to the Te NWs on the paper due to the applied voltage, Raman spectra of the nanowire-coated paper were recorded before and after the experiment. Three kinds of samples (neutral species, positively charged species, and negatively charged species) were analyzed continuously for 25 min, and Raman spectra of the paper were recorded before and after analysis. These spectra (Figure 5) showed a prominent peak due to the Raman active  $A_1$  singlet mode of the t-Te lattice vibration.<sup>26</sup> The other peaks at 267 and 375  $\text{cm}^{-1}$  are due to various vibrational modes of Te–O bond.<sup>27</sup> These were collected at various points on the paper to ascertain reproducibility. For a better presentation of the Raman spectra before and after experiments, a vertical shift of spectra has been done. There may be a small intensity variation in the spectrum before and after the experiment. That variation in the intensity is due to the changes in the experimental parameters, like the focus spot for Raman measurement, the amount of NWs present at that point (can be seen from the FE SEM images that the NWs concentration is not same at all the points), and so forth. There is no physical degradation seen for the NWs. The data suggest that the Te NWs are unchanged in the course of the experiment.

The experiments presented suggest that ionization does not lead to changes in the electrodes. Tellurium being a semiconductor, application of a potential at the electrode surface should result in a potential drop. We measured a

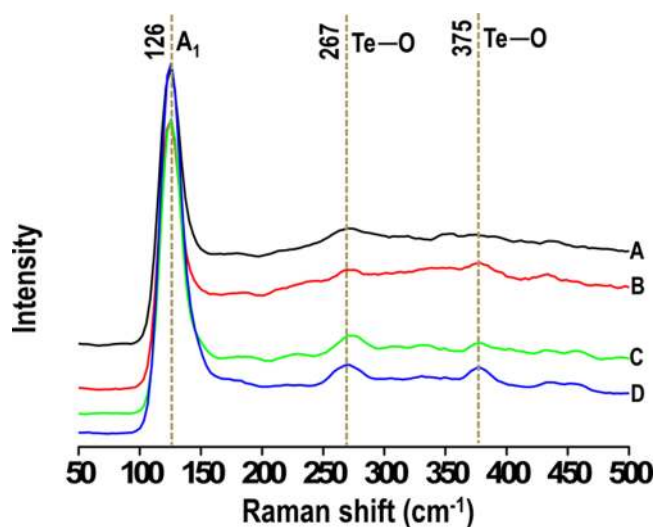


**Figure 5.** Raman spectra of tellurium-coated paper. (A) Before the experiment, after the experiment for (B) neutral molecules, (C) positive counterpart of a preformed ion, and (D) negative counterpart of a preformed ion. The spectra have been shifted vertically for clarity.

potential drop of 0.40 V upon the application of 1 V on the NWs-coated paper (Supporting Information, SI-3). The existence of ions even under these conditions implies that ion formation is unlikely to be occurring at this reduced potential at the end of the NWs (opposite to the point of electrical contact). Similar to our previous report,<sup>19</sup> experiments with vapors introduced between the electrodes and the mass spectrometer inlet did not produce ions. Creation of ions from solutions and their detection as preformed ions imply ionization in solution, and emission presumably as microdroplets. Conduction seems to involve ions in the solution covering the NWs and droplet emission occurs from the end of the wet electrode where the field is highest. This is supported by the enhancement of ion signals in acidic pH for a range of analytes.

In order to verify the mechanism of ionization, solutions of the same analyte (DPA) were prepared in a homologous series of alcohols with decreasing dielectric constant. Although ions were detected in methanol and ethanol, they were not detectable in butanol and only with substantial reduction in intensity in propanol (see Table S1). These findings highlight the key role of solvents in the ionization mechanism. The mechanism of ionization was tested with another experiment for which solutions of DPA (50 ppm) in butanol with varying conductivity were prepared. This was done by adding an external ionic species, at different concentrations, to the analyte system. Butanol solution of sodium acetate was prepared and was added to the analyte solutions so that the final salt concentrations were 1, 10, 50, 100, and 500 ppm. Mass spectra were collected, and the signal intensity is listed in Table S2. Ions were not detectable up to 50 ppm concentration of sodium acetate (in the analyte system), but ionization started occurring at 100 ppm of sodium acetate. This is ascribed to the enhancement of electrolytic conductivity of the analyte system. This confirms the role of electrolytic conductivity of the solution in ejecting ions from NWs. Electronic conductivity of the nanostructure does not seem to be important. This is supported by the fact that the nature of carbon nanotubes, whether single-walled or multiwalled, did not make a difference in ionization.<sup>19</sup>

The dependence of alignment of these nanostructures on molecular ion intensity has been tested with various analytes. To do this, the aligned tellurium nanowire suspension was transferred on to a square cut silicon (001) single crystal substrate and analysis of various molecules was done with the silicon substrate in different positions (from position 1 to 8 as shown in Figure 6A). Alignment of NWs was checked with

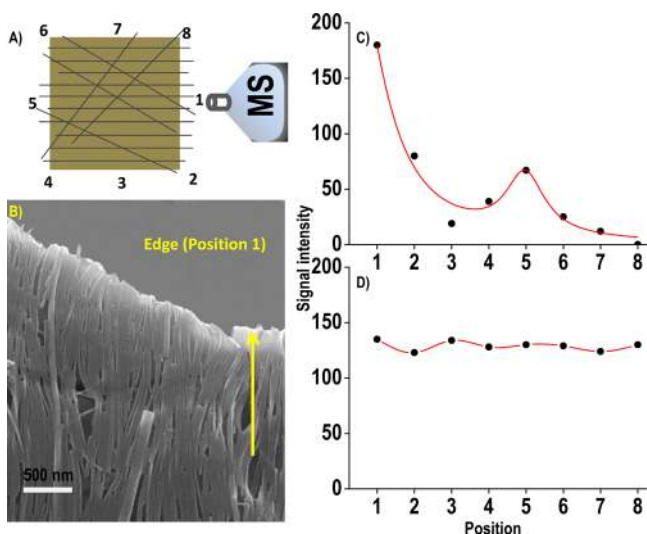


**Figure 6.** Analysis of TPP at different positions of a silicon (001) single crystal substrate coated with Te NWs. (A) Schematic of the silicon substrate showing different positions (from 1 to 8) which are analyzed consecutively, (B) microscopic image of the silicon substrate coated with aligned Te NWs. At the edge of the Si substrate, the Te NWs would bend downward. Variation in ion intensity of triphenylphosphine collected from (C) aligned Te NWs, and (D) nonaligned Te NWs, both deposited on silicon substrates. Some disorder in the alignment of NWs is shown.

SEM imaging. The substrate with aligned Te NWs was held in front of the MS inlet at an approximate distance of 1 mm, and it was rotated repeatedly in steps of approximately  $45^\circ$  anticlockwise with respect to the MS inlet. The rotation caused different regions of the substrate to face the MS inlet in turn. Measurements were done with various analytes. Results for a set of experiments using TPP are shown in Figure 6C, and others are given in Figure 7. There is a large variation in molecular ion intensity at different positions of the silicon

substrate. In particular, we note that positions 1 and 5 have much larger intensities than others. Analysis of these particular regions under a microscope revealed the difference in alignment of nanostructures in these positions with respect to the MS inlet. The microscopic image is shown in Figure 6B.

The edge of the silicon substrate is marked in the image, and the alignment of nanostructures is shown by an arrow. The positions where ion intensity got enhanced are those at which nanowire alignment is along the axis of the MS inlet. Other regions where intensity is less are those where NWs lie at an angle with respect to the mass spectrometer inlet. At certain positions, most of the NWs are orthogonal to the mass spectrometer inlet. However, even in these positions, certain NWs will be protruding from the substrate oriented toward the inlet as would be expected from Figures 1B and 1D. This makes a gradual variation in ion intensity with positions with maxima at 0 and  $180^\circ$  with respect to the MS inlet.

Positions 1 and 5 are edges of the substrate cut that the tips of NWs facing the MS inlet. The Te NWs at these positions are 8  $\mu\text{m}$  in length and 10 nm in diameter. These are distributed over a 4 mm long edge (the substrate dimension is  $4 \times 4$  mm). So there can be  $4 \times 10^5$  wires over the entire edge (assuming monolayer coating). The distribution of NWs is unlikely to be the same at positions 1 and 5, because they are nanoscale materials and the monolayer is made by solution casting. There is difference in morphology as well as number density between these positions (Figure S4A). These contribute to variations in the ion intensity at apparently equivalent positions such as 1 and 5 as well as 7 and 3. To confirm the existence of anisotropy in such ionization events we performed measurements with a variety of analytes as well as varying substrates. The results show the reproducibility of the main finding of anisotropy in the experiment. These data are shown in Figure S5 and S6. The difference in arrangement of NWs can be understood from microscopy, in general as seen in Figure 1B. Nearly similar intensities are observed upon reversal of electrode positions. Because precise position control was not possible in these experiments (note that the control possible in electrode alignment is much smaller than the dimensions of NWs), the observed alignment-dependent intensity variation was confirmed by performing similar measurements with a silicon substrate deposited with nonaligned Te NWs (Figure S4B). In this case, all positions have almost equal intensity. Data using TPP are shown in Figure 6D, and similar results for other analytes are presented in Figure 7. Signal intensity data of DPA

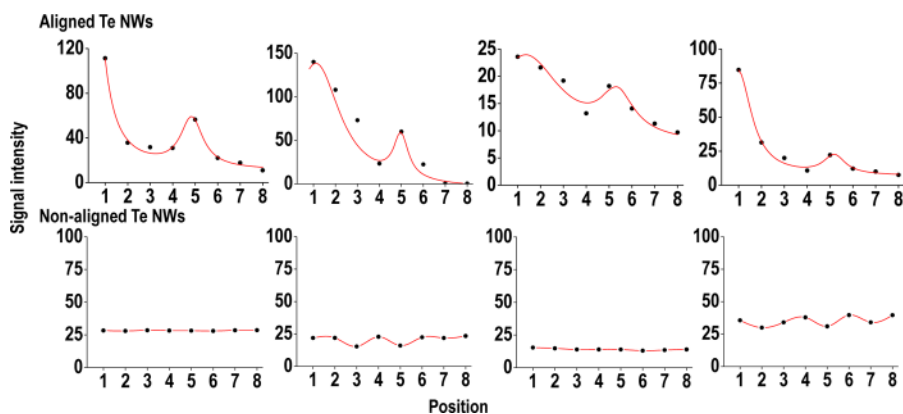


**Figure 7.** Variation of signal intensity with different orientations of the TeNWs: aligned (top) and nonaligned (bottom) for (A) diphenylamine, (B) isoleucine, (C) threonine, and (D) phenyl alanine. Positions are as in Figure 6.

as a function of position for both types of Te NWs are shown in Table S3.

Because it was difficult to accurately reproduce the position of the substrate containing Te NWs with respect to the entrance to the mass spectrometer, the effects of applied potential were explored by switching from 1 to 0 V keeping other conditions the same. Similarly, orientation was studied under two extreme conditions of parallel and orthogonal. These experiments were done at various pH values for DPA, thymine, adenine, and guanine, and the results are summarized in the Supporting Information, Table S4. These data confirm that (i) there is a significant orientation effect (an order of magnitude or more), (ii) there is an increase in ion signal of about a factor of 2 on going from 0 to 1 V, and (iii) there is a significant pH effect with acidic solutions strongly favoring observation of  $[M + H]^+$ .

The applicability of this low-voltage ionization has been tested with various analytes. These include amino acids, pesticides, and drugs. The zwitterionic nature of amino acids allows them to exist in solution as charged species. Ionization of these species was achieved at 1 V from Te NWs-coated paper, and the result of an experiment using phenylalanine is shown in Figure 8A. The spectrum is dominated by the protonated

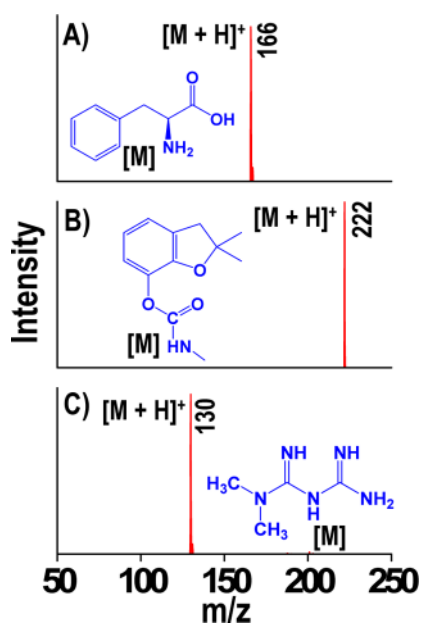


**Figure 8.** Detection of (A) amino acid (phenyl alanine), (B) carbofuran (from the surface of an orange), and (C) content of a medicinal tablet (metformin) at 1 V.

molecule peak at  $m/z$  166. This study was extended to various amino acids ranging from alanine ( $m/z$  90) to methionine ( $m/z$  150) as shown in Figure S7. Similarly, various pesticides were studied. Pesticides at 50 ppm concentration were applied on the surface of an orange. The rectangle of nanowire-coated paper was rubbed on the orange surface and solvent (methanol/water) added, and mass spectra were collected at 1 V. The spectrum of carbofuran recorded in this way is shown in Figure 8B. The result suggests the possibility of detecting 250 ng of pesticides from fruit surfaces. Results for various pesticides are shown in Figure S8. The figure shows mass spectrum of chlorpyrifos, parathion, and methyl parathion with their  $MS^2$  data, confirming their identity. The ultralow

voltage ionization method has been extended to identify the contents of various medicinal tablets also. A number of tablets were purchased from a local pharmacy, and the tablet surface was rubbed with the Te NWs-coated paper and analyzed using methanol/water at 1 V. Figure 8C presents the mass spectrum of metformin which was analyzed from a metformin tablet. Various other tablets were analyzed and the signal intensity data are given in Table S5.

## CONCLUSIONS

In conclusion, we present a widely applicable low voltage ionization process involving one-dimensional nanostructures. Ionized molecular species are detected without accompanying fragment ions. It is shown that ionization is independent of the substrate used for the nanostructures. Ion formation occurs as a result of the enhanced electric fields at the tips of the nanostructures causing charged droplet emission. Electrolytic conduction in solution over the nanostructures is found to be the basis for conductivity. Alignment of nanostructures with respect to the mass spectrometer inlet has a significant effect on ion intensity. The observed anisotropy is ascribed to the effects of NW alignment on the electric field direction, but it might also contain contributions from physical flow profiles across the oriented NWs. High sensitivity and selectivity to the molecular species expressed on surfaces offer certain analytical advantages to this methodology. Simplification of mass spectrometry ionization is possible using easily prepared nanostructures. The data also indicate that there are processes that produce ions at zero applied potential; these processes are studied in a separate publication.<sup>28</sup>

## ASSOCIATED CONTENT

### Supporting Information

The Supporting Information is available free of charge on the ACS Publications website at DOI: 10.1021/acs.analchem.5b01596.

Additional information as noted in text (PDF)

## AUTHOR INFORMATION

### Corresponding Authors

\*E-mail: pradeep@iitm.ac.in. Fax: (+) 91-44-22570545.

\*E-mail: cooks@purdue.edu.

### Notes

The authors declare no competing financial interest.

## ACKNOWLEDGMENTS

T.P. acknowledges financial support from the Department of Science and Technology, Government of India, for his research programme on nanomaterials. R.N. and D.S. thank the University Grants Commission for research fellowships. A.S. thanks CSIR for a research fellowship. R.G.C. acknowledges funding from the Separations and Analysis Program, Office of Basic Energy Sciences, U.S. Department of Energy, DE-FG02-06ER15807.

## REFERENCES

- (1) Beckey, H. D. *Int. J. Mass Spectrom. Ion Phys.* **1969**, *2*, 500–503.
- (2) Robertson, A. J. B. *J. Phys. E: Sci. Instrum.* **1974**, *7*, 321.
- (3) Hsu, C. S. *Prepr. Symp. Am. Chem. Soc., Div. Fuel Chem.* **2011**, *56*, 421.
- (4) Takats, Z.; Wiseman, J. M.; Gologan, B.; Cooks, R. G. *Science* **2004**, *306*, 471–473.

- (5) Zhang, J.; Huo, F.; Zhou, Z.; Bai, Y.; Liu, H. *Huaxue Jinzhan* **2012**, *24*, 101–109.
- (6) Takats, Z.; Cotte-Rodriguez, I.; Talaty, N.; Chen, H.; Cooks, R. G. *Chem. Commun.* **2005**, 1950–1952.
- (7) Zhang, X.; Wang, N.; Zhou, Y.; Liu, Y.; Zhang, J.; Chen, H. *Anal. Methods* **2013**, *5*, 311–315.
- (8) Monge, M. E.; Harris, G. A.; Dwivedi, P.; Fernandez, F. M. *Chem. Rev.* **2013**, *113*, 2269–2308.
- (9) Ifá, D. R.; Wu, C.; Ouyang, Z.; Cooks, R. G. *Analyst* **2010**, *135*, 669–681.
- (10) Huang, M.-Z.; Cheng, S.-C.; Cho, Y.-T.; Shiea, J. *Anal. Chim. Acta* **2011**, *702*, 1–15.
- (11) Harris, G. A.; Galhena, A. S.; Fernandez, F. M. *Anal. Chem.* **2011**, *83*, 4508–4538.
- (12) Watrous, J. D.; Alexandrov, T.; Dorrestein, P. C. *J. Mass Spectrom.* **2011**, *46*, 209–222.
- (13) *Ambient Ionization Mass Spectrometry*; Domin, M.; Cody, R., Eds.; Royal Society of Chemistry: London, U.K., 2015; Vol. 2.
- (14) Liu, J.; Wang, H.; Manicke, N. E.; Lin, J.-M.; Cooks, R. G.; Ouyang, Z. *Anal. Chem.* **2010**, *82*, 2463–2471.
- (15) Cody, R. B.; Dane, A. J. *Rapid Commun. Mass Spectrom.* **2014**, *28*, 893–898.
- (16) Yang, Q.; Wang, H.; Maas, J. D.; Chappell, W. J.; Manicke, N. E.; Cooks, R. G.; Ouyang, Z. *Int. J. Mass Spectrom.* **2012**, *312*, 201–207.
- (17) Sarkar, D.; Sen Gupta, S.; Narayanan, R.; Pradeep, T. *J. Am. Soc. Mass Spectrom.* **2014**, *25*, 380–387.
- (18) Liu, J.; Manicke, N. E.; Zhou, X.; Cooks, R. G.; Ouyang, Z. *New Dev. Mass Spectrom.* **2015**, *2*, 389–422.
- (19) Narayanan, R.; Sarkar, D.; Cooks, R. G.; Pradeep, T. *Angew. Chem., Int. Ed.* **2014**, *53*, 5936–5940.
- (20) Porcari, A. M.; Fernandes, G. D.; Belaz, K. R. A.; Schwab, N. V.; Santos, V. G.; Alberici, R. M.; Gromova, V. A.; Eberlin, M. N.; Lebedev, A. T.; Tata, A. *Anal. Methods* **2014**, *6*, 2436–2443.
- (21) Douglass, K. A.; Venter, A. R. *J. Mass Spectrom.* **2013**, *48*, 553–560.
- (22) Qian, H. S.; Yu, S. H.; Gong, J. Y.; Luo, L. B.; Fei, L. F. *Langmuir* **2006**, *22*, 3830–3835.
- (23) Moon, G. D.; Lee, T. I.; Kim, B.; Chae, G. S.; Kim, J.; Kim, S. H.; Myoung, J.-M.; Jeong, U. *ACS Nano* **2011**, *5*, 8600–8612.
- (24) Xu, X.; Lu, W.; Cole, R. B. *Anal. Chem.* **1996**, *68*, 4244–4253.
- (25) Wang, G.; Cole, R. B. *Anal. Chim. Acta* **2000**, *406*, 53–65.
- (26) Pine, A. S.; Dresselhaus, G. *Phys. Rev. B* **1971**, *4*, 356–371.
- (27) Samal, A. K.; Pradeep, T. *J. Phys. Chem. C* **2009**, *113*, 13539–13544.
- (28) Wleklinski, M.; Li, Y.; Bag, S.; Narayanan, R.; Sarkar, D.; Pradeep, T.; Cooks, R. G. *Anal. Chem.* **2015**, *87*, 6786.